



# Optimization of the synthesis conditions for LaNiO<sub>3</sub> catalyst by microwave assisted citrate method for hydrogen production

Ahmed Galal\*, Nada F. Atta, Shima M. Ali

Department of Chemistry, Faculty of Science, Cairo University, 12613 Giza, Egypt

## ARTICLE INFO

### Article history:

Received 28 May 2011

Received in revised form 2 October 2011

Accepted 3 October 2011

Available online 8 October 2011

### Keywords:

Perovskites

Catalysis

Nanoparticles

Hydrogen evolution

Microwave synthesis

## ABSTRACT

LaNiO<sub>3</sub> was prepared by microwave assisted citrate method. The effect of the synthesis condition such as, the operating microwave power and the microwave irradiation time, on structural, surface and catalytic properties was investigated by XRD, SEM, Tafel linear polarization and impedance measurements. The XRD results suggested successful incorporation of Ni<sup>3+</sup> at the La<sup>3+</sup> cations sites confirming the formation of the hexagonal distorted rhombohedral perovskite phase of LaNiO<sub>3</sub> at all the investigated microwave operating powers and irradiation times. The average particle size ranges between 18 and 32 nm. The largest surface area (*ca.* 25 m<sup>2</sup> g<sup>-1</sup>) and the highest catalytic activity for LaNiO<sub>3</sub> prepared by the microwave assistant-citrate method toward the hydrogen evolution reaction (HER) were obtained at an operating microwave power of 720 W and increased by increasing the microwave irradiation time. In addition, the reaction order, the activation energy and the reaction mechanism were identified.

© 2011 Elsevier B.V. All rights reserved.

## 1. Introduction

The hydrogen evolution reaction (HER) is an attractive reaction that illustrates the importance of research in the field of renewable energy. There is a significant technological interest in this reaction due to its important role in electrodeposition and corrosion of metals in acids, in storage of energy via hydrogen production, and as the microscopic reverse of the hydrogen oxidation reaction in low-temperature fuel cells [1–3]. The electrocatalysis in the HER is one of the most important subjects in the field of electrochemistry. Three properties play an important role in selecting catalytically active materials for hydrogen evolution: (a) actual intrinsic electrocatalytic effect of the material, (b) large active surface area per unit volume ratio (both of which are directly related to the overpotential used to operate the electrolyzer at significant current densities) and (c) catalyst stability [4]. Thus, from an electrochemical point of view, the problem to be tackled in order to decrease the cost of electrolytic hydrogen is the reduction of overpotentials. The desired decrease in overpotential can be achieved by choosing catalytically efficient active electrode materials, or by increasing the active surface area of the electrode.

Nickel metal is among the best candidates for HER. The electrocatalytic activity of nickel for the HER can be enhanced by the modification of the electronic structure of the electrode metal by alloying or by the use of some suitable preparation method.

Perovskite-type oxides, have the general formula ABO<sub>3</sub> (A: alkaline earth or lanthanide, responsible for the thermal resistance; B: transition element, responsible for catalytic activity) when subjected to redox processes, perovskite-type oxides produce very small particles, in the order of nanometers, with high metallic dispersion [5,6] thus, providing the best matrix for many transition metal catalysts. The efficient use of these catalyst precursors requires a high dispersion of the metal phase, which can be achieved by controlled segregation of the active phase. It is also well established that the synthesis method plays an important role in the catalytic performance. The different synthesis methods generate structural, surface and textural changes in the properties of the materials, influencing their catalytic behavior [7,8].

The microwave irradiation process (MIP), which is one of the novel processes evolved from microwave sintering, was widely applied in inorganic/organic synthesis, food drying, microwave-induced catalysis and plasma chemistry. With its rapid development in recent decades, MIP has obtained a growing interest, especially in material synthesis research. The advantages of MIP can be summarized as: (i) rapid reaction velocity; (ii) uniform heating; (iii) clean and energy efficient. During the past years, many perovskites such as GaAlO<sub>3</sub>, LaCrO<sub>3</sub>, etc., have been reported to be synthesized by MIP for their ferroelectricity, superconductivity, high-temperature ionic conductivity, or a variety of magnetic ordering [9–11]. It was reported that smaller grain size and more rapid lattice diffusion would be formed when using microwave synthesis route than other wet chemical processes [12], which might enhance the lattice oxygen mobility in catalysis process. However, secondary phases were formed during the perovskite synthesis

\* Corresponding author. Tel.: +20 35676561, fax: +20 35727556.

E-mail addresses: [galal@sci.cu.edu.eg](mailto:galal@sci.cu.edu.eg), [galalah1@yahoo.com](mailto:galalah1@yahoo.com) (A. Galal).

by MIP [13] and the average particle size obtained was relatively higher than that obtained by other conventional synthesis methods such as sol–gel method.

In this work,  $\text{LaNiO}_3$  is prepared by microwave assisted citrate method. This method combined the advantages of both MIP and citrate–nitrate method. As a single-phase perovskite of uniform particle size distribution, small average particle size (in the nanometer scales) and enhanced catalytic properties are obtained. The synthesis conditions are optimized in order to achieve the best catalytic activity. The electrocatalytic activity toward HER is investigated by Tafel and electrochemical impedance measurements. A complete kinetics study is carried out in which the reaction order, the activation energy and the reaction mechanism are determined.

## 2. Experimental

### 2.1. Chemicals

Lanthanum(III) nitrate hexahydrate (Sigma–Aldrich, puriss. p.a., 99%), Nickel(II) nitrate hexahydrate (Bio Basic INC, 98–102%), citric acid, nitric acid, sulfuric acid, ammonia (Aldrich), graphite powder (Sigma–Aldrich, <20  $\mu\text{m}$ , synthetic) and paraffin oil (Fluka) were used as received without further purification. All solutions were prepared using double distilled water. All measurements were made in oxygen-free solution, which was achieved by continuous purging of the cell electrolyte with nitrogen gas (99.999% pure).

### 2.2. Catalyst preparation

Stoichiometric amounts of La-nitrate and Ni-nitrate were weighed, dissolved in distilled water and stirred for 5 min. To this aqueous solution, a sufficient amount of citric acid was added so that the molar ratio of citric acid to total metal ions is 1:1. The solution was stirred well for uniform mixing. Ammonia was added to adjust the pH of the solution at 8. The solution was placed in a conventional microwave oven and the reaction was performed under ambient atmosphere for 30 min. The microwave was operated in 30-s cycles (20 s on, 10 s off). The precursor complex dehydrated and became more viscous with time producing a dark gel. The gel got ignited giving a voluminous fluffy powder. A ceramic nano-oxide was then obtained by calcinating at temperature of ca. 900 °C.

### 2.3. Electrochemical cell and equipments

A standard three-electrode, one compartment cell was used in all experiments. A two compartment cell separated by a porous plug was also used to ensure the absence of any diffusion effect from the oxidation or reduction products at the anode or cathode. Since no evidence was observed for any change in the studied trend, all experiments were conducted in the standard one compartment cell. The platinum counter electrode has a large surface area. The reference electrode was a commercially available saturated silver/silver chloride electrode. The working electrode was a carbon paste electrode (CPE) ( $d=0.63$  cm), the unmodified CPE was prepared as follows: 0.125 g of reagent grade graphite powder was used, washed with acetone, dried and then mixed with 45  $\mu\text{L}$  of paraffin oil. To modify the CPE, the graphite powder was mixed with the modifier in 10% (w/w%). Both unmodified and modified carbon pastes were packed through the Teflon holder that had been cut and leveled at the end. Electrical contact to the paste was established via a thin copper rod passed through of the Teflon holder. With a clean weighing paper, fresh surfaces were obtained by polishing the electrodes until they showed a smooth and shiny appearance after every measurement.

All electrochemical measurements, the DC polarization and the electro-chemical impedance spectroscopy (EIS), were carried out in

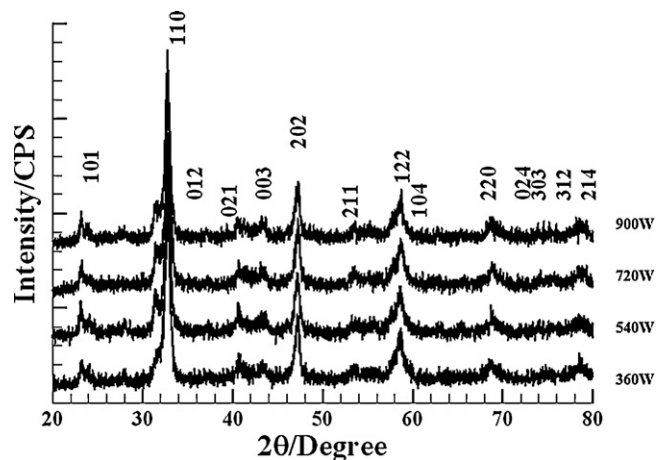


Fig. 1. XRD patterns of  $\text{LaNiO}_3$  prepared by microwave assisted citrate method at different operating microwave powers for 20 min. Miller indices ( $h, l, k$ ) are given.

0.1 M  $\text{H}_2\text{SO}_4$  aqueous acid using a Gamry-750 system and a lock-in-amplifier that are connected to a personal computer.

DC polarization measurements of hydrogen evolution were carried out by first stabilizing the electrode at open-circuit potential (OCP) until a steady-state OCP value was obtained (usually about 30 min). The typical electrode was then conditioned at  $-0.2$  V for 10 min and at  $-0.3$  V for 5 min. A typical linear polarization measurement was conducted from  $-0.3$  V to  $-0.6$  V, at a scan rate of  $1 \text{ mVs}^{-1}$ . The DC polarization measurement was followed by a set of electrochemical impedance spectroscopy measurements at selected overpotentials.

The order of the reaction with respect to  $\text{H}^+$  was determined at constant ionic strength of the solution by varying the  $\text{H}_2\text{SO}_4$  concentration between 0.05 M and 0.5 M (6 solutions), keeping the ionic strength constant with  $\text{Na}_2\text{SO}_4$ . Only one DC polarization measurement was taken at each  $\text{H}_2\text{SO}_4$  concentration by the same procedure mentioned above.

### 2.4. Catalyst characterization

The scanning electron microscopy analysis was performed by using a Philips XL30 and X-ray diffraction analysis was obtained using Shimadzu XRD-700 instruments. Surface area measurements were achieved using Autosorb-6B surface area and pore size analyzer.

## 3. Results and discussion

### 3.1. The effect of the operating microwave power

Lanthanum nickel oxide,  $\text{LaNiO}_3$  was prepared by microwave assistant-citrate method. The prepared catalyst was tested for the HER. The influence of the synthesis conditions (the microwave power and the microwave irradiation time) on the surface area, structural and catalytic properties was investigated. The effect of the microwave power was studied by heating the lanthanum–nickel citrate complex in a microwave oven operating at  $x$  W ( $x=360, 540, 720$  and  $900$  W) for 20 min in repeated 30 s cycles. The prepared samples, after being calcined, were characterized by X-ray powder diffractograms. Fig. 1 shows the XRD of  $\text{LaNiO}_3$  prepared by microwave assistant-citrate method at different operating microwave powers. The results suggested successful incorporation of  $\text{Ni}^{3+}$  at the  $\text{La}^{3+}$  cations sites confirming the formation of the hexagonal distorted rhombohedral perovskite phase of  $\text{LaNiO}_3$  for all the investigated operating microwave powers.

**Table 1**  
Structural parameters calculated from XRD data.

	Crystal structure	BET ( $\text{m}^2 \text{g}^{-1}$ )	Average particle size (nm)	Lattice parameters ( $\text{\AA}$ )	Lattice volume ( $\text{\AA}^3$ )	Theoretical density ( $\text{g/cm}^3$ )
Standard	Hexagonal distorted rhombohedral			$a = 5.456$ $c = 6.572$	169.42	7.22
LaNiO <sub>3</sub>	Hexagonal distorted rhombohedral	10.68	18.2	$a = 4.113$ $c = 6.583$	96.44	12.69
360 W	Hexagonal distorted rhombohedral			$a = 4.116$ $c = 6.578$	95.51	12.68
LaNiO <sub>3</sub>	Hexagonal distorted rhombohedral	7.97	24.5	$a = 4.110$ $c = 6.591$	96.43	12.69
540 W	Hexagonal distorted rhombohedral			$a = 4.118$ $c = 6.586$	96.71	12.65
LaNiO <sub>3</sub>	Hexagonal distorted rhombohedral	25.26	20.1	$a = 4.122$ $c = 6.619$	97.39	12.56
720 W	Hexagonal distorted rhombohedral			$a = 4.110$ $c = 6.591$	96.43	12.69
LaNiO <sub>3</sub>	Hexagonal distorted rhombohedral	7.18	22.0	$a = 4.117$ $c = 6.544$	96.06	12.74
900 W	Hexagonal distorted rhombohedral			$a = 4.112$ $c = 6.577$	96.31	12.70
LaNiO <sub>3</sub>	Hexagonal distorted rhombohedral	21.14	32.4			
15 min	Hexagonal distorted rhombohedral					
LaNiO <sub>3</sub>	Hexagonal distorted rhombohedral	25.26	20.1			
20 min	Hexagonal distorted rhombohedral					
LaNiO <sub>3</sub>	Hexagonal distorted rhombohedral	150.59	22.2			
25 min	Hexagonal distorted rhombohedral					
LaNiO <sub>3</sub>	Hexagonal distorted rhombohedral	383.30	19.8			
30 min	Hexagonal distorted rhombohedral					

Important structural parameters were also calculated from XRD data such as, particle size, lattice parameters, lattice volume and theoretical density [14]. These parameters together with the surface area measured by the BET method were calculated and listed in Table 1. There is a deviation in the calculated ( $a$ ) value from that of the standard which in turn caused a deviation in the values of the lattice volume and density. This is may be due to the distortion in the rhombohedral phase. At ambient conditions LaNiO<sub>3</sub> crystallizes in a rhombohedrally distorted perovskite structure with space group  $R\bar{3}c$ . With respect to the ideal cubic  $Pm\bar{3}m$  structure

this rhombohedral structure is obtained by an anti-phase tilt of the adjacent NiO<sub>6</sub> octahedra about the  $[1\ 1\ 1]_p$  pseudocubic diagonal, described by the  $a$ - $a$ - $a$  tilt system in Glazer's notation [15]. The aristotype cubic phase of LaNiO<sub>3</sub> is susceptible to octahedral rotations because of an underbonded La–O coordination. Similar to other rhombohedrally distorted perovskites, LaNiO<sub>3</sub> undergoes a temperature-induced rhombohedral-to-cubic phase transition upon heating: the NiO<sub>6</sub> octahedral rotation angle  $\theta$  reduces continuously to zero in the cubic phase. In the  $R\bar{3}c$ , the La cations occupy the  $2a$  ( $\frac{1}{4}, \frac{1}{4}, \frac{1}{4}$ ) Wyckoff positions while the Ni cations occupy the

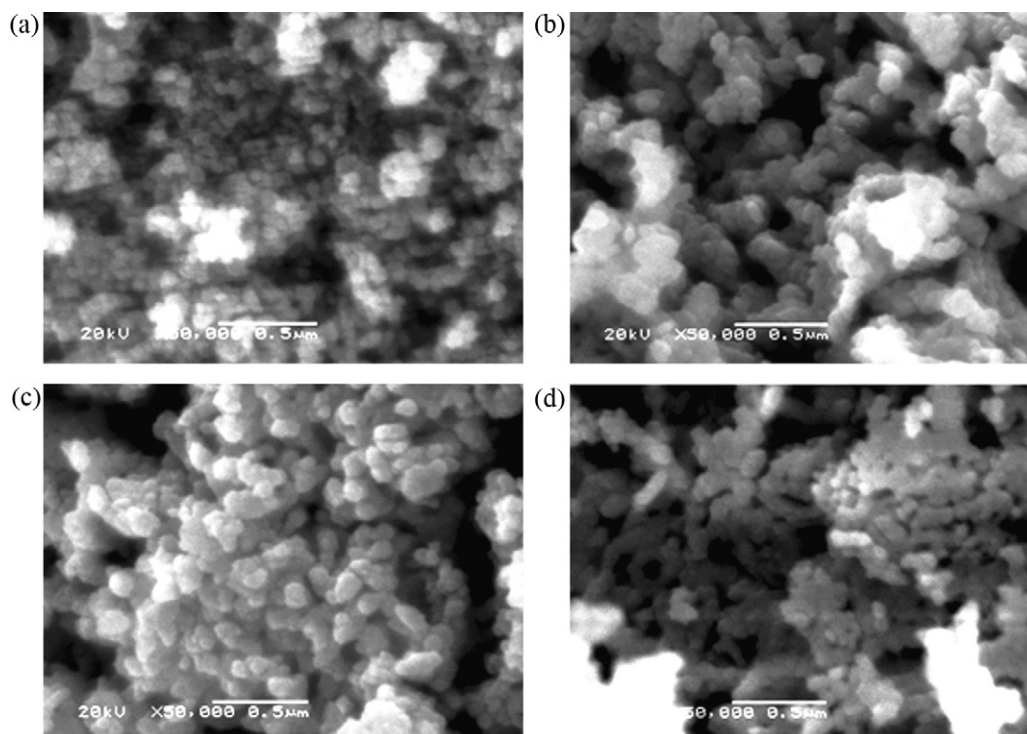


**Fig. 2.** SEM micrographs of LaNiO<sub>3</sub> prepared by microwave assisted citrate method at (a) 360 W, (b) 540 W, (c) 720 W and (d) 900 W for 20 min. With a magnification of 50,000 times.

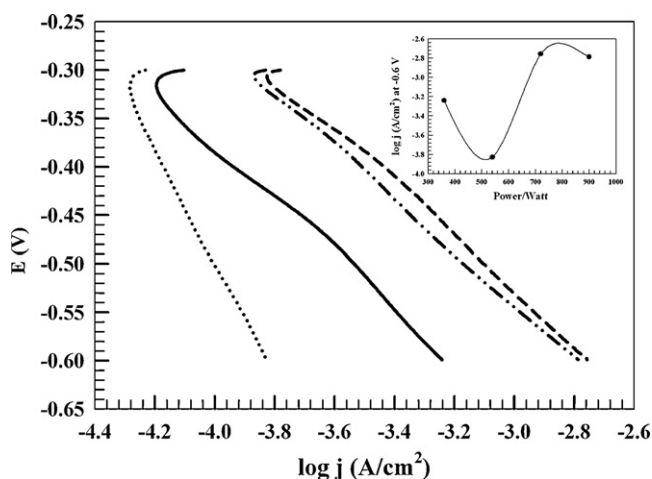


**Fig. 3.** Linear Tafel polarization curves for the HER recorded on CPE modified with 10% (w/w%)  $\text{LaNiO}_3$  prepared by microwave assisted citrate method at different operating microwave powers for 20 min in 0.1 M  $\text{H}_2\text{SO}_4$ , scan rate =  $1 \text{ mV s}^{-1}$ . (—) 360 W, (···) 540 W, (---) 720 W and (- · - ·) 900 W. The inset represents the dependence of the rate of the HER (the current density normalized to the geometric area of the electrode) on the operating microwave power.

2b (0; 0; 0) positions. The oxygen atoms are at the  $6e(x, x^- + 1/4, 1/2)$  where  $x$  is the only free internal structural parameter that sets the rotation angle of the  $\text{NiO}_6$  octahedra [16].

It can also be shown that the particle size was not affected greatly by changing the operating microwave power. However, the surface area of the prepared perovskites changed. The microwave power of 720 W provided the largest surface area ( $25.26 \text{ m}^2 \text{ g}^{-1}$ ) and showed a distinct morphology as indicated from the SEM images.

The morphology of the prepared perovskites was studied by SEM. Fig. 2 shows the SEM images of  $\text{LaNiO}_3$  prepared by microwave assistant-citrate method at different microwave operating powers (a) 360 W, (b) 540 W, (c) 720 W and (d) 900 W. The SEM images showed that the operating microwave power does not affect the morphology of the resulting perovskites greatly. The prepared perovskites are composed of agglomerations of particles of irregular shape and rough surface except at 720 W, a well-defined crystalline morphology with the largest surface area was observed. In conclusion, by changing the operating microwave power, the particle size values are indeed comparable and also the surface area values except in case of sample prepared at 720 W which has a higher surface area of  $25 \text{ m}^2 \text{ g}^{-1}$ . This can be explained from SEM images as the morphology of this sample is different from others, where the appearance of well defined semi-spherical grains. For a film 320 nm thick the roughness factor is 24 nm.

The electrocatalytic activity of the prepared perovskites toward HER was investigated by Tafel linear polarization measurements. Fig. 3 shows a set of Tafel lines recorded in 0.1 M  $\text{H}_2\text{SO}_4$  in the potential region of hydrogen evolution for carbon paste electrodes modified with 10% (w/w%)  $\text{LaNiO}_3$  prepared by microwave assistant-citrate method at different operating microwave powers. The inset shows the dependence of the measured current due to HER on the operating microwave power. By considering this region of potential, the calculated values of the Tafel slope, exchange current density, and transfer coefficient for the prepared perovskites were calculated and listed in Table 2. The Tafel slope values indicated that the Volmer reaction step is the rate determining step. It could also be noticed that the Tafel slope and transfer coefficient values deviated from the theoretical values ( $116 \text{ mV decade}^{-1}$  and 0.5, respectively) [17–19]. This phenomenon has already been reported in the literature [17] and has been explained as a characteristic feature for oxide catalysts. Considering

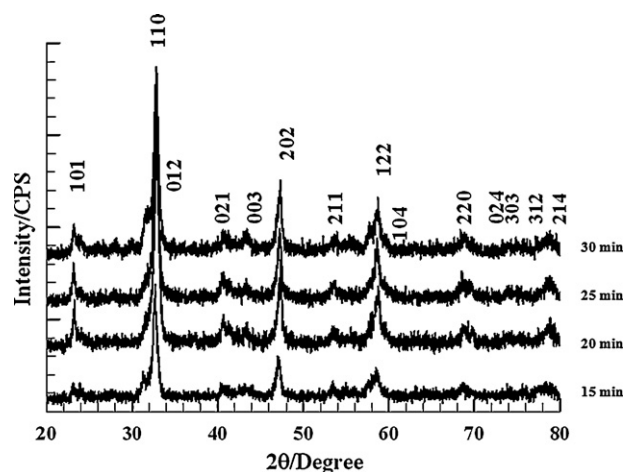


**Fig. 4.** XRD patterns of  $\text{LaNiO}_3$  prepared by microwave assisted citrate method at an operating microwave power of 720 W for different microwave irradiation times. Miller indices ( $h, l, k$ ) are given.

the exchange current density values, which is directly proportional to the reaction rate at equilibrium, presented in Table 2, it can be concluded that the electrocatalytic activity of  $\text{LaNiO}_3$  prepared at different operating microwave powers increased in the order of  $720 > 900 > 360 > 540 \text{ W}$ . Although, a value of exchange current density is frequently used for the characterization of electrocatalytic activity, it has been reported that values of Tafel slope and transfer coefficient in the low overpotential region were as or even more important than a favorable exchange current density value [20]. This is due to the fact that the HER does not occur at a reversible potential (i.e. zero overpotential), but a certain overpotential is required for the reaction to proceed at a measurable rate. Hence, in order to compare the electrocatalytic activity of the catalysts prepared by different methods at the conditions relevant for the operation of hydrogen generator, a given current density value (i.e. where hydrogen production is achieved at a given rate) and compare the corresponding overpotentials required to reach the given current density value. This should give an indication on the amount of energy (overpotential) that is used to produce a specified amount of hydrogen (since the current is, through the Faraday law, is directly related to the amount of the produced hydrogen). Thus, the current density values are measured at a fixed overpotential of  $-300 \text{ mV}$  and the overpotential values are measured at current density of  $0.5 \text{ mA cm}^{-2}$ . From the data presented in Table 2, it is concluded that the largest surface area and the highest catalytic activity for HER was for  $\text{LaNiO}_3$  prepared by the microwave assistant-citrate method was obtained at an operating microwave power of 720 W.

### 3.2. The effect of the microwave irradiation time

The effect of the microwave irradiation time was studied by heating the lanthanum–nickel citrate complex in a microwave oven operating at 720 W for  $x$  min ( $x = 15, 20, 25$  and 30) in 30 s-cycles. The prepared samples, after being calcined, were characterized by X-ray powder diffractograms. Fig. 4 shows the XRD of  $\text{LaNiO}_3$  prepared by microwave assistant-citrate method at different microwave irradiation times. The results suggested successful incorporation of  $\text{Ni}^{3+}$  at the  $\text{La}^{3+}$  cations sites confirming the formation of the hexagonal distorted rhombohedral perovskite phase of  $\text{LaNiO}_3$  at all the investigated microwave irradiation times.

The structural parameters calculated from XRD data together with the surface area measured by the BET method are calculated and listed in Table 1. It can be shown that changing the operating microwave irradiation time affected both the particle size and

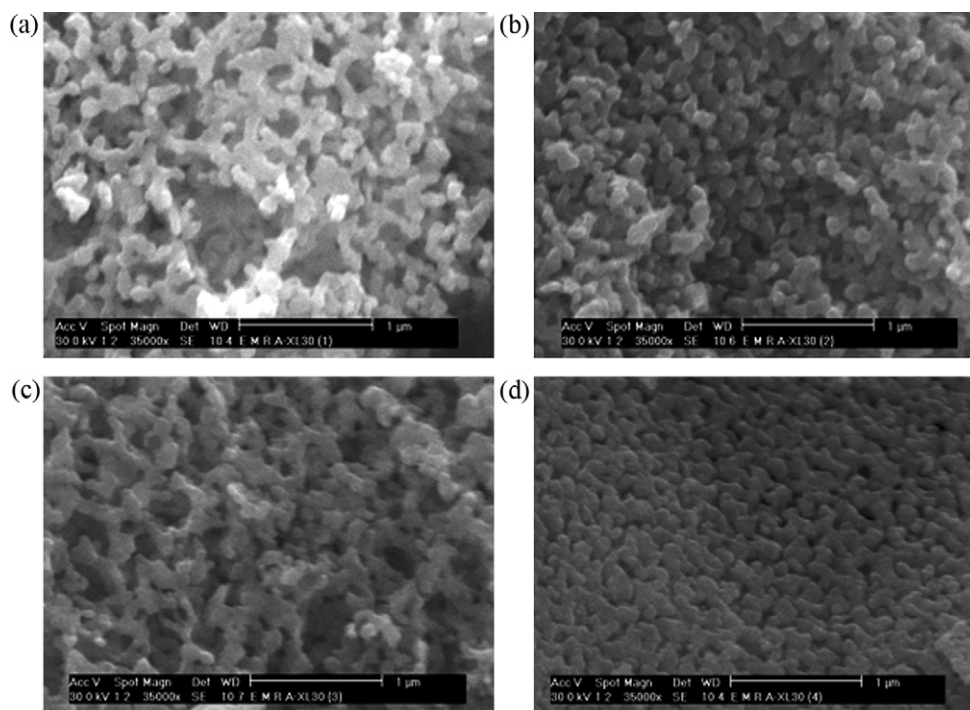


**Fig. 5.** SEM micrographs of LaNiO<sub>3</sub> prepared by microwave assisted citrate method at an operating microwave power of 720 W for (a) 15 min, (b) 20 min, (c) 25 min and (d) 30 min. With a magnification of 35,000 times.

the surface area of the prepared perovskites to a great extent. The microwave irradiation time that provided the largest surface area and the smallest particle size was obtained by heating the complex for 30 min, which is also revealed in the SEM images.

The morphology of the prepared perovskites was studied by SEM. Fig. 5 shows the SEM images of LaNiO<sub>3</sub> prepared by microwave assistant-citrate method at a microwave irradiation time of (a) 15 min, (b) 20 min, (c) 25 min and (d) 30 min. It can be noticed that the microwave irradiation time affected the morphology of the prepared perovskites. At the beginning, for particles prepared at irradiation times 15 and 20 min, the particles are grouped in frameworks containing pores that are filled with particles agglomerations at this stage, leading to the formation of a relatively condensed and compact surface. Further increasing of the microwave irradiation time, *ca.* 25 min, led to the formation of a second layer of particle frameworks over a compact background. At a microwave irradiation time of 30 min, the particles are relatively ordered and a highly compact surface was observed. Pore distribution, shown by SEM images, reflects the change in surface area values.

The electrocatalytic activity of the prepared perovskites for HER was investigated by Tafel linear polarization measurements. Fig. 6 shows the Tafel lines recorded in 0.1 M H<sub>2</sub>SO<sub>4</sub> in the potential region of hydrogen evolution for carbon paste electrodes modified with 10% (w/w%) LaNiO<sub>3</sub> prepared by microwave assistant-citrate method at different microwave irradiation times. The inset shows

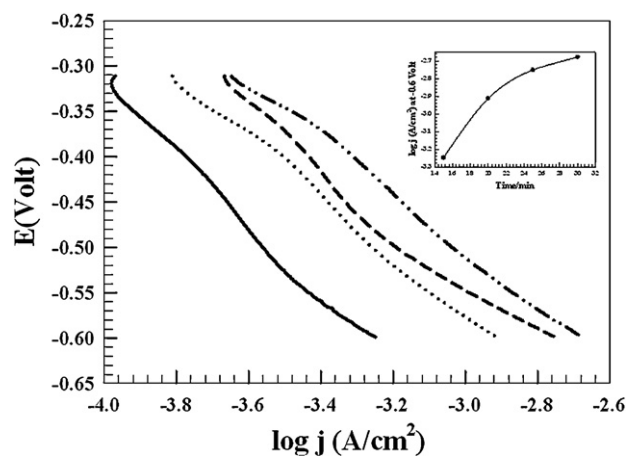


**Fig. 6.** Linear Tafel polarization curves for the HER recorded on CPE modified with 10% (w/w%) LaNiO<sub>3</sub> prepared by microwave assisted citrate method at an operating microwave power of 720 W for different microwave irradiation times in 0.1 M H<sub>2</sub>SO<sub>4</sub>, scan rate = 1 mV s<sup>-1</sup>. The inset represents the dependence of the rate of the HER (the current density normalized to the geometric area of the electrode) on the microwave irradiation time.

**Table 2**

HER kinetics parameters obtained by analysis of Linear Tafel polarization curves for LaNiO<sub>3</sub> prepared by the microwave-assistant citrate method.

	$b$ (mV dec <sup>-1</sup> )	$j_0$ ( $\mu$ A cm <sup>-2</sup> )	$A$	$j$ ( $\mu$ A cm <sup>-2</sup> ) at $-300$ mV	$\eta$ (mV) at $0.5$ mA/cm <sup>-2</sup>
360 W	381.4	-4.61	0.15	-78.87	-507
540 W	501.7	-1.50	0.12	-58.61	>-600
720 W	336.3	-12.24	0.18	-158.50	-390
900 W	350.2	-10.67	0.17	-141.25	-404
15 min	349.6	-1.35	0.17	-100.01	-529
20 min	336.3	-12.24	0.18	-158.50	-390
25 min	334.5	-13.04	0.18	-223.87	-371
30 min	315.9	-15.84	0.19	-251.19	-339

**Table 3**

HER kinetics parameters obtained by analysis of Linear Tafel polarization curves for LaNiO<sub>3</sub> prepared by the microwave-assistant citrate method calculated at different temperatures.

T (K)	b (mV dec <sup>-1</sup> )	j <sub>0</sub> (μA cm <sup>-2</sup> )	α
298	317.7	-10.52	0.1856
308	336.3	-12.24	0.1831
318	344.8	-68.71	0.1824
328	367.0	-77.37	0.1768
338	381.6	-164.41	0.1752

the dependence of the cathodic current on the microwave irradiation time. The calculated values of Tafel slope, exchange current density, and transfer coefficient for the prepared perovskites are calculated and listed in Table 2. Again, the Tafel slope values indicated that the Volmer reaction step is the rate determining step. Considering the exchange current density values, presented in Table 2, it can be concluded that the catalytic activity for HER increases by increasing the microwave irradiation time used in the preparation of perovskites. Also, both the current density values, measured at a fixed overpotential of -300 mV and the overpotential values, measured at current density of 0.5 mA cm<sup>-2</sup>, which were presented in Table 2, showed comparable trend to that obtained with the exchange current density. Thus, the optimum synthesis conditions, applied for all perovskites prepared by the microwave assisted citrate method, were an operating microwave power of 720 W and a microwave irradiation time of 30 min.

### 3.3. Order of reaction with respect to H<sup>+</sup>

The order of the reaction with respect to H<sup>+</sup> was determined at constant ionic strength of the solution by varying the H<sub>2</sub>SO<sub>4</sub> concentration keeping the ionic strength constant with Na<sub>2</sub>SO<sub>4</sub>. Only one DC polarization measurement was taken at each H<sub>2</sub>SO<sub>4</sub> concentration by the same procedure as described in the experimental section. The reaction order value of LaNiO<sub>3</sub> prepared by microwave assistant-citrate method was 0.94. The fractional reaction order was expected for HER catalyzed by oxide catalysts [21].

### 3.4. Activation energy

In order to evaluate the temperature effect on the kinetics of the HER for the catalysts prepared by different methods, DC linear polarization (Tafel) measurements were done for a wide temperature range, from 298 K to 338 K. The activation energy value for LaNiO<sub>3</sub> was 51.61 kJ mol<sup>-1</sup>. This value was very close to those usually postulated for HER occurring through the Heyrovsky mechanism [22]. Savadogo et al. obtained values ranging from 36 kJ mol<sup>-1</sup> to 56 kJ mol<sup>-1</sup> on Pt-Co supported on carbon at zero overpotential, while Giz et al. [23] reported a value of 39 kJ mol<sup>-1</sup> on NiZn. A higher value, 62 kJ mol<sup>-1</sup> was reported on NiFeZn [24].

The corresponding electrochemical parameters Tafel slopes and transfer coefficients together with the exchange current densities at various temperatures were calculated and listed in Table 3. It can be shown that the transfer coefficient values for HER decreased

**Table 4**

The electrical equivalent circuit parameters calculated from the NLLS analysis for LaNiO<sub>3</sub> prepared by the microwave-assistant citrate method.

η (V)	Rs (Ω cm <sup>2</sup> )	CPE1 (F cm <sup>-2</sup> )	m	R1 (Ω cm <sup>2</sup> )	CPE2 (F cm <sup>-2</sup> )	n	R2 (Ω cm <sup>2</sup> )
-0.025	6.50	59,953.84	0.91	18538.73	15.16	0.04	57.66
-0.050	8.79	63,951.94	0.92	15425.45	18.90	0.07	20.84
-0.075	9.14	65,272.97	0.92	9768.49	11.39	0.06	933.63
-0.100	8.40	68,873.08	0.92	8722.98	11.80	0.06	920.40
-0.125	10.39	72,250.56	0.93	7675.27	11.37	0.09	635.58
-0.150	10.42	74,698.08	0.93	6184.04	11.34	0.09	697.96

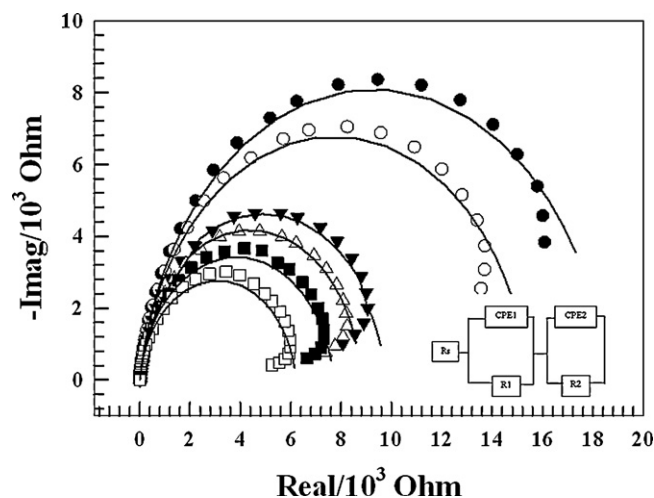


**Fig. 7.** Nyquist plots showing an EIS response of CPEs modified with 10% LaNiO<sub>3</sub> prepared by microwave assisted citrate method in 0.1 M H<sub>2</sub>SO<sub>4</sub> at various HER overpotentials: -25 mV (●), -50 mV (○), -75 mV (▼), -100 mV (△), -125 mV (■) and -150 mV (□), symbols are experimental and solid lines are modeled data, the inset represents Electrical equivalent circuit used to explain the EIS response.

with temperature. This behavior has already been reported in literature for HER on Ni electrode [25].

### 3.5. Electrochemical impedance spectroscopy

To ensure a complete characterization of the electrode/electrolyte interface and corresponding processes, EIS measurements were conducted over a frequency range from 100 kHz to 10 mHz at selected overpotentials from the DC polarization curves. Experimental EIS data were modeled using non-linear least-squares fit analysis (NLLS) software and electrical equivalent circuit. Fig. 7 shows a set of EIS spectra recorded on carbon paste electrode modified with 10% (w/w%) LaNiO<sub>3</sub> prepared by microwave assistant-citrate method at various overpotentials. The data showed that the experimental (symbols) and simulated (lines) data are in very good agreement at all the overpotentials investigated when the equivalent circuit shown in the inset was used to describe the EIS response of the investigated catalyst. This model has been used to describe the response of the HER on porous electrodes [26]. It reflects the response of a HER system characterized by two time constants, only one of them (CPE1) is related to the kinetics of the HER. This time constant changes with overpotential. The second time constant (CPE2) is related to the porosity of the electrode surface, and does not change with overpotential. Fig. 7 shows that the radius of the high-frequency semicircle (smaller semicircle) was potential independent, it can be related to the electrode surface porosity response, while the radius of the low frequency semicircle (larger semicircle) decreased with an increase in overpotential, was then related to the charge transfer resistance process and double layer capacitance. Studies of the HER on solid electrodes [18] showed that when the radius of the high frequency semicircle (smaller semicircle) is

potential-independent, it can be related to the electrode surface porosity, while the potential-dependent low-frequency semicircle (larger semicircle) is then related to the charge transfer resistance process and double layer capacitance. Table 4 shows the electrical equivalent circuit parameters calculated from NLLS analysis for  $\text{LaNiO}_3$  prepared by microwave assistant-citrate method. With an increase in overpotential, there were two results, first CPE1 increased and R1 decreased too so, it can be concluded that the (CPE1-R1) was related to the HER charge-transfer kinetics, namely to the response of double layer capacitance characterized by CPE1 and HER charge transfer resistance characterized by R1. The second result was in contrary to the behavior of CPE1, the value of CPE2 was shown to be relatively constant. At the same time, the value of R2 decreased. This is a typical behavior related to the porosity of the electrode surface.

This EIS behavior is quite in consistence with the Tafel behavior discussed previously. As from the Tafel measurements, the slow rate determining step in the HER on the carbon paste electrodes modified with perovskites was the adsorption of hydrogen (Volmer), while the desorption step was fast. Consequently, the absence of an EIS hydrogen adsorption time constant could be expected, as also confirmed by the EIS measurements. This demonstrates that although EIS and Tafel techniques are two quite different experimental techniques, results obtained by both techniques are comparable.

#### 4. Conclusion

$\text{LaNiO}_3$  was successfully prepared by microwave assisted citrate method. Optimization of the synthesis conditions was performed in order to obtain the highest possible catalytic activity for HER. By changing the operating microwave power the particle size did not affect greatly. However, the surface area of the prepared perovskites did well which suggested different morphologies of samples prepared at different operating microwave powers as shown by the SEM images. The microwave power that provided the largest surface area and the highest catalytic activity of  $\text{LaNiO}_3$  prepared by microwave assisted citrate method for the HER was 720 W. The catalyst performance is excellent even with the expected resistance that ranges between 4 and  $100 \Omega \text{ cm}^{-1}$  [27]. While the surface area and the catalytic activity for HER increased by increasing the microwave irradiation time. The calculated value of the reaction order for hydrogen evolution at  $\text{LaNiO}_3$  prepared by microwave assistant-citrate method was 0.94 and the activation energy value was  $51.61 \text{ kJ mol}^{-1}$ . The slow rate determining step in the HER on

the carbon paste electrode modified with  $\text{LaNiO}_3$  perovskite was the adsorption of hydrogen (Volmer) as indicated from both Tafel and impedance measurements.

#### Acknowledgment

The authors would like to express their gratitude to Cairo University through the office of the Vice President for Graduate Studies and Research for the partial financial support.

#### References

- [1] M. Hamson, W. Colella, D. Golden, *Science* 308 (2005) 1901–1905.
- [2] C. Hamann, A. Hamnett, W. Vielstich, *Electrochemistry*, Wiley-VCH, Weinheim, 1998.
- [3] CRC Handbook of Chemistry and Physics, CRC Press, New York, 1996.
- [4] F. Elisa, O. Sasha, *J. Mol. Catal. A: Chem.* 242 (2005) 182–194.
- [5] M. Goldwasser, M. Rivas, E. Pietri, M. Pérez-Zurita, M. Cubeiro, M. Griboval-Constant, G. Leclercq, *J. Mol. Catal. A: Chem.* 228 (2005) 325–331.
- [6] G. Valderrama, M. Goldwasser, M. Urbina, J. Tatibouët, J. Barrault, C. Batiot-Dupeyrat, F. Martínez, *Catal. Today* 107 (2005) 785–791.
- [7] A. Norman, M. Morris, *J. Mater. Process Technol.* 92–93 (1999) 91–96.
- [8] A. Galal, S. Darwish, N.N. Atta, S. Ali, A. El Fatah, *Appl. Catal. A: Gen.* 378 (2010) 151–159.
- [9] M. Selvam, K. Rao, *Adv. Mater.* 12 (2000) 1621–1624.
- [10] K. Gibbons, S. Blundell, A. Mihut, I. Gameson, P. Edwards, Y. Miyazaki, N. Hyatt, M. Jones, A. Porch, *Chem. Commun.* 1 (2000) 159–160.
- [11] M. Selvam, K. Rao, *J. Mater. Chem.* 13 (2003) 596–601.
- [12] H. Yan, X. Huang, Z. Lu, H. Huang, R. Xue, L. Chen, *J. Power Sources* 68 (1997) 530–532.
- [13] R. Ran, D. Weng, X. Wu, J. Fan, L. Qing, *Catal. Today* 126 (2007) 394–399.
- [14] B. Cullity, *Elements of X-ray diffraction*, 2nd ed., Addison Wiley Publication Company, USA, 1978.
- [15] Chaban, N. Weber, M. Pignard, S. Kreisel, *J. Appl. Phys. Lett.* 97 (2010) 031915–31923.
- [16] G. Gou, I. Grinberg, A.M. Rappe, J.M. Rondinelli, *Science* (2011) 14, ar X iv: 1105.0198.
- [17] Southampton Electrochemistry Group, *Instrumental Methods in Electrochemistry*, Wiley, New York, 1985.
- [18] B. Borresen, G. Hagen, R. Tunold, *Electrochim. Acta* 47 (2002) 1819–1827.
- [19] E. Ndzebet, O. Savadogo, *Int. J. Hydrogen Energy* 20 (1995) 635–640.
- [20] R. Simpraga, G. Tremiliosi-Filho, S. Qian, B. Conway, *J. Electroanal. Chem.* 424 (1997) 141–151.
- [21] E. Fachinotti, E. Guerrini, A. Tavares, S. Trasatti, *J. Electroanal. Chem.* 600 (2007) 103–112.
- [22] E. Ndzebet, O. Savadogo, *Int. J. Hydrogen Energy* 26 (2001) 213–218.
- [23] M. Giz, S. Machado, L. Avaca, E. Gonzalez, *J. Appl. Electrochem.* 22 (1992) 973–977.
- [24] M. Giz, S. Bento, E. Gonzalez, *Int. J. Hydrogen Energy* 25 (2000) 621–626.
- [25] N. Krstajic, M. Popovic, B. Brgur, M. Vojnovic, D. Sepa, *J. Electroanal. Chem.* 515 (2001) 27–33.
- [26] D. Spena, in: J.O'M. Bockris, B.E. Conway, R.E. White (Eds.), *Modern Aspects of Electrochemistry*, vol. 29, Springer, Germany, 1996.
- [27] J. Choi, J. Ryu, B. Hahn, W. Yoon, D. Park, *J. Am. Ceram. Soc.* 91 (2008) 2756–2758.